EUROPEAN ORGANIZATION FOR NUCLEAR RESEARCH

CERN-EP-2000-101
20 July 2000

W^+W^- Production Cross Section and W Branching Fractions in e^+e^- Collisions at 189 GeV

The OPAL Collaboration

Abstract

From a data sample of 183 pb^{-1} recorded at a center-of-mass energy of $\sqrt{s} = 189$ GeV with the OPAL detector at LEP, 3068 W-pair candidate events are selected. Assuming Standard Model W boson decay branching fractions, the W-pair production cross section is measured to be σ_{WW}=16.30 $\pm$ 0.34(stat.) $\pm$ 0.18(syst.) pb. When combined with previous OPAL measurements, the W boson branching fraction to hadrons is determined to be 68.32 $\pm$ 0.61(stat.) $\pm$ 0.28(syst.) % assuming lepton universality. These results are consistent with Standard Model expectations.

(Submitted to Physics Letters B)

The OPAL Collaboration

G. Abbiendi[2], K. Ackerstaff[8], C. Ainsley[5], P.F. Åkesson[3], G. Alexander[22], J. Allison[16], K.J. Anderson[9], S. Arcelli[17], S. Asai[23], S.F. Ashby[1], D. Axen[27], G. Azuelos[18,a], I. Bailey[26], A.H. Ball[8], E. Barberio[8], R.J. Barlow[16], S. Baumann[3], T. Behnke[25], K.W. Bell[20], G. Bella[22], A. Bellerive[9], G. Benelli[2], S. Bentvelsen[8], S. Bethke[32], O. Biebel[32], I.J. Bloodworth[1], O. Boeriu[10], P. Bock[11], J. Böhme[14,h], D. Bonacorsi[2], M. Boutemeur[31], S. Braibant[8], P. Bright-Thomas[1], L. Brigliadori[2], R.M. Brown[20], H.J. Burckhart[8], J. Cammin[3], P. Capiluppi[2], R.K. Carnegie[6], A.A. Carter[13], J.R. Carter[5], C.Y. Chang[17], D.G. Charlton[1,b], P.E.L. Clarke[15], E. Clay[15], I. Cohen[22], O.C. Cooke[8], J. Couchman[15], C. Couyoumtzelis[13], R.L. Coxe[9], A. Csilling[15,j], M. Cuffiani[2], S. Dado[21], G.M. Dallavalle[2], S. Dallison[16], A. de Roeck[8], E. de Wolf[8], P. Dervan[15], K. Desch[25], B. Dienes[30,h], M.S. Dixit[7], M. Donkers[6], J. Dubbert[31], E. Duchovni[24], G. Duckeck[31], I.P. Duerdoth[16], P.G. Estabrooks[6], E. Etzion[22], F. Fabbri[2], M. Fanti[2], L. Feld[10], P. Ferrari[12], F. Fiedler[8], I. Fleck[10], M. Ford[5], A. Frey[8], A. Fürtjes[8], D.I. Futyan[16], P. Gagnon[12], J.W. Gary[4], G. Gaycken[25], C. Geich-Gimbel[3], G. Giacomelli[2], P. Giacomelli[8], D. Glenzinski[9], J. Goldberg[21], C. Grandi[2], K. Graham[26], E. Gross[24], J. Grunhaus[22], M. Gruwé[25], P.O. Günther[3], C. Hajdu[29], G.G. Hanson[12], M. Hansroul[8], M. Hapke[13], K. Harder[25], A. Harel[21], M. Harin-Dirac[4], A. Hauke[3], M. Hauschild[8], C.M. Hawkes[1], R. Hawkings[8], R.J. Hemingway[6], C. Hensel[25], G. Herten[10], R.D. Heuer[25], J.C. Hill[5], A. Hocker[9], K. Hoffman[8], R.J. Homer[1], A.K. Honma[8], D. Horváth[29,c], K.R. Hossain[28], R. Howard[27], P. Hüntemeyer[25], P. Igo-Kemenes[11], K. Ishii[23], F.R. Jacob[20], A. Jawahery[17], H. Jeremie[18], C.R. Jones[5], P. Jovanovic[1], T.R. Junk[6], N. Kanaya[23], J. Kanzaki[23], G. Karapetian[18], D. Karlen[6], V. Kartvelishvili[16], K. Kawagoe[23], T. Kawamoto[23], R.K. Keeler[26], R.G. Kellogg[17], B.W. Kennedy[20], D.H. Kim[19], K. Klein[11], A. Klier[24], S. Kluth[32], T. Kobayashi[23], M. Kobel[3], T.P. Kokott[3], S. Komamiya[23], R.V. Kowalewski[26], T. Kress[4], P. Krieger[6], J. von Krogh[11], T. Kuhl[3], M. Kupper[24], P. Kyberd[13], G.D. Lafferty[16], H. Landsman[21], D. Lanske[14], I. Lawson[26], J.G. Layter[4], A. Leins[31], D. Lellouch[24], J. Letts[12], L. Levinson[24], R. Liebisch[11], J. Lillich[10], B. List[8], C. Littlewood[5], A.W. Lloyd[1], S.L. Lloyd[13], F.K. Loebinger[16], G.D. Long[26], M.J. Losty[7], J. Lu[27], J. Ludwig[10], A. Macchiolo[18], A. Macpherson[28,m], W. Mader[3], S. Marcellini[2], T.E. Marchant[16], A.J. Martin[13], J.P. Martin[18], G. Martinez[17], T. Mashimo[23], P. Mättig[24], W.J. McDonald[28], J. McKenna[27], T.J. McMahon[1], R.A. McPherson[26], F. Meijers[8], P. Mendez-Lorenzo[31], W. Menges[25], F.S. Merritt[9], H. Mes[7], A. Michelini[2], S. Mihara[23], G. Mikenberg[24], D.J. Miller[15], W. Mohr[10], A. Montanari[2], T. Mori[23], K. Nagai[8], I. Nakamura[23], H.A. Neal[12,f], R. Nisius[8], S.W. O'Neale[1], F.G. Oakham[7], F. Odorici[2], H.O. Ogren[12], A. Oh[8], A. Okpara[11], M.J. Oreglia[9], S. Orito[23], G. Pásztor[8,j], J.R. Pater[16], G.N. Patrick[20], J. Patt[10], P. Pfeifenschneider[14,i], J.E. Pilcher[9], J. Pinfold[28], D.E. Plane[8], B. Poli[2], J. Polok[8], O. Pooth[8], M. Przybycień[8,d], A. Quadt[8], C. Rembser[8], P. Renkel[24], H. Rick[4], N. Rodning[28], J.M. Roney[26], S. Rosati[3], K. Roscoe[16], A.M. Rossi[2], Y. Rozen[21], K. Runge[10], O. Runolfsson[8], D.R. Rust[12], K. Sachs[6], T. Saeki[23], O. Sahr[31], E.K.G. Sarkisyan[22], C. Sbarra[26], A.D. Schaile[31], O. Schaile[31], P. Scharff-Hansen[8], M. Schröder[8], M. Schumacher[25], C. Schwick[8], W.G. Scott[20], R. Seuster[14,h], T.G. Shears[8,k], B.C. Shen[4], C.H. Shepherd-Themistocleous[5], P. Sherwood[15], G.P. Siroli[2], A. Skuja[17], A.M. Smith[8], G.A. Snow[17], R. Sobie[26], S. Söldner-Rembold[10,e], S. Spagnolo[20], M. Sproston[20], A. Stahl[3], K. Stephens[16], K. Stoll[10], D. Strom[19], R. Ströhmer[31], L. Stumpf[26], B. Surrow[8], S.D. Talbot[1], S. Tarem[21], R.J. Taylor[15], R. Teuscher[9], M. Thiergen[10], J. Thomas[15], M.A. Thomson[8], E. Torrence[9], S. Towers[6], D. Toya[23], T. Trefzger[31], I. Trigger[8], Z. Trócsányi[30,g], E. Tsur[22], M.F. Turner-Watson[1], I. Ueda[23], B. Vachon26, P. Vannerem[10], M. Verzocchi[8], H. Voss[8], J. Vossebeld[8], D. Waller[6], C.P. Ward[5], D.R. Ward[5], P.M. Watkins[1], A.T. Watson[1], N.K. Watson[1], P.S. Wells[8], T. Wengler[8], N. Wermes[3], D. Wetterling[11] J.S. White[6], G.W. Wilson[16], J.A. Wilson[1], T.R. Wyatt[16], S. Yamashita[23], V. Zacek[18], D. Zer-Zion[8,l]

[1]School of Physics and Astronomy, University of Birmingham, Birmingham B15 2TT, UK

[2]Dipartimento di Fisica dell' Università di Bologna and INFN, I-40126 Bologna, Italy
[3]Physikalisches Institut, Universität Bonn, D-53115 Bonn, Germany
[4]Department of Physics, University of California, Riverside CA 92521, USA
[5]Cavendish Laboratory, Cambridge CB3 0HE, UK
[6]Ottawa-Carleton Institute for Physics, Department of Physics, Carleton University, Ottawa, Ontario K1S 5B6, Canada
[7]Centre for Research in Particle Physics, Carleton University, Ottawa, Ontario K1S 5B6, Canada
[8]CERN, European Organisation for Nuclear Research, CH-1211 Geneva 23, Switzerland
[9]Enrico Fermi Institute and Department of Physics, University of Chicago, Chicago IL 60637, USA
[10]Fakultät für Physik, Albert Ludwigs Universität, D-79104 Freiburg, Germany
[11]Physikalisches Institut, Universität Heidelberg, D-69120 Heidelberg, Germany
[12]Indiana University, Department of Physics, Swain Hall West 117, Bloomington IN 47405, USA
[13]Queen Mary and Westfield College, University of London, London E1 4NS, UK
[14]Technische Hochschule Aachen, III Physikalisches Institut, Sommerfeldstrasse 26-28, D-52056 Aachen, Germany
[15]University College London, London WC1E 6BT, UK
[16]Department of Physics, Schuster Laboratory, The University, Manchester M13 9PL, UK
[17]Department of Physics, University of Maryland, College Park, MD 20742, USA
[18]Laboratoire de Physique Nucléaire, Université de Montréal, Montréal, Quebec H3C 3J7, Canada
[19]University of Oregon, Department of Physics, Eugene OR 97403, USA
[20]CLRC Rutherford Appleton Laboratory, Chilton, Didcot, Oxfordshire OX11 0QX, UK
[21]Department of Physics, Technion-Israel Institute of Technology, Haifa 32000, Israel
[22]Department of Physics and Astronomy, Tel Aviv University, Tel Aviv 69978, Israel
[23]International Centre for Elementary Particle Physics and Department of Physics, University of Tokyo, Tokyo 113-0033, and Kobe University, Kobe 657-8501, Japan
[24]Particle Physics Department, Weizmann Institute of Science, Rehovot 76100, Israel
[25]Universität Hamburg/DESY, II Institut für Experimental Physik, Notkestrasse 85, D-22607 Hamburg, Germany
[26]University of Victoria, Department of Physics, P O Box 3055, Victoria BC V8W 3P6, Canada
[27]University of British Columbia, Department of Physics, Vancouver BC V6T 1Z1, Canada
[28]University of Alberta, Department of Physics, Edmonton AB T6G 2J1, Canada
[29]Research Institute for Particle and Nuclear Physics, H-1525 Budapest, P O Box 49, Hungary
[30]Institute of Nuclear Research, H-4001 Debrecen, P O Box 51, Hungary
[31]Ludwigs-Maximilians-Universität München, Sektion Physik, Am Coulombwall 1, D-85748 Garching, Germany
[32]Max-Planck-Institute für Physik, Föhring Ring 6, 80805 München, Germany

[a] and at TRIUMF, Vancouver, Canada V6T 2A3
[b] and Royal Society University Research Fellow
[c] and Institute of Nuclear Research, Debrecen, Hungary
[d] and University of Mining and Metallurgy, Cracow
[e] and Heisenberg Fellow
[f] now at Yale University, Dept of Physics, New Haven, USA
[g] and Department of Experimental Physics, Lajos Kossuth University, Debrecen, Hungary
[h] and MPI München
[i] now at MPI für Physik, 80805 München
[j] and Research Institute for Particle and Nuclear Physics, Budapest, Hungary
[k] now at University of Liverpool, Dept of Physics, Liverpool L69 3BX, UK
[l] and University of California, Riverside, High Energy Physics Group, CA 92521, USA
[m] and CERN, EP Div, 1211 Geneva 23.

1 Introduction

In 1996, the LEP collider at CERN entered a new phase of operation, LEP2, with the first e^+e^- collisions above the W^+W^- production threshold at $\sqrt{s} = 161$ GeV. By 1998, with the installation of additional super-conducting radio-frequency accelerating cavities, the center-of-mass collision energy of the LEP collider was increased to $\sqrt{s} = 189$ GeV. This paper describes the measurement of the W^+W^- production cross section and the W boson branching fractions using 183 pb^{-1} of data recorded by the OPAL detector during the 1998 LEP run. This measurement provides an important test of the non-Abelian nature of the electroweak interaction, as the W^+W^- production cross section above threshold is sensitive to the couplings between the weak gauge bosons. In addition, with the large sample of W bosons produced in 1998, more precise tests of the weak charged-current interaction can be made in the measurement of the W boson branching fractions to leptons and hadrons.

In the Standard Model, W^+W^- events are expected to decay into fully leptonic ($W^+W^- \to \ell^+\nu_\ell\ell'^-\overline{\nu}_{\ell'}$), semi-leptonic ($W^+W^- \to q\overline{q}\ell^\pm\nu_\ell$), or fully hadronic ($W^+W^- \to q\overline{q}q\overline{q}$) final states with predicted branching fractions of 10.6%, 43.9%, and 45.6% respectively [1]. Three separate selections, described in Sections 3–5, are used in this analysis to identify candidate W^+W^- events by their final state topologies. For the $\ell\nu\ell\nu$ and $qq\ell\nu$ event selections, events are further classified according to charged lepton type. In total, W^+W^- candidate events are exclusively selected in one of ten possible final states ($6 \times \ell\nu\ell\nu$, $3 \times qq\ell\nu$, and $1 \times qqqq$).

From the observed event rates in these ten channels, measurements of the W boson branching fractions and the total W^+W^- production cross section are performed as described in Section 6. The branching fraction measurements at $\sqrt{s} = 189$ GeV are also combined with previous OPAL results from data collected at $\sqrt{s} = 161$ GeV [2], $\sqrt{s} = 172$ GeV [3], and $\sqrt{s} = 183$ GeV [4].

2 Data and Monte Carlo Models

The OPAL detector has been described in detail in previous publications [5]. The data reconstruction, luminosity measurement, Monte Carlo models, and detector simulation used for this analysis are identical to those used in previous OPAL W^+W^- cross-section measurements [3, 4]. The accepted integrated luminosity, evaluated using small angle Bhabha scattering events observed in forward calorimeters, is $183.05 \pm 0.16(\text{stat.}) \pm 0.37(\text{syst.})$ pb^{-1} [6]. The mean center-of-mass energy for the data sample is $\sqrt{s} = 188.635 \pm 0.040$ GeV [7].

The semi-analytic program GENTLE 2.0 [8] has been used to calculate the W^+W^- cross section $\sigma_{WW} = 16.65$ pb at $\sqrt{s} = 188.635$ GeV assuming a W boson mass of $M_W = 80.41$ GeV [9]. The estimated theoretical uncertainty on the GENTLE prediction is 2%. Recent theoretical calculations which include a more complete treatment of $\mathcal{O}(\alpha)$ radiative corrections through the double pole approximation [10] are now available in the YFSWW [11] and RACOONWW [12] Monte Carlo generators. These new calculations predict a W^+W^- cross section of 16.27 pb and 16.25 pb respectively, with a reduced theoretical uncertainty of 0.42%. Even though YFSWW and RACOONWW differ in their implementation of $\mathcal{O}(\alpha)$ radiative corrections, these two calculations are in agreement at the level of 0.1%, and predict a rate which is (2.3–2.4)% lower than the older GENTLE estimate.

A W^+W^- cross section of 16.26 ± 0.08 pb is used throughout this paper to determine the expected number of W^+W^- events predicted by the Standard Model. This value is chosen to be representative of these improved calculations, while covering the expected range of theoretical uncertainty quoted by either YFSWW or RACOONWW.

A number of additional Monte Carlo generators are used in this analysis to provide estimates of signal efficiencies and expected backgrounds from other Standard Model processes. Unless otherwise noted, all Monte Carlo event samples have been processed through a detailed simulation of the OPAL detector [13].

In this paper, W^+W^- events are defined in terms of the CC03 class of production diagrams shown in Figure 1 following the notation of [1]. These amplitudes, namely the t-channel ν_e exchange and s-channel Z^0/γ exchange, provide a natural definition of resonant W-pair production, even though other non-CC03 diagrams contribute to the same four-fermion final states. The efficiency for selecting CC03 signal events is estimated using the KORALW 1.42 [14] Monte Carlo generator, with the predictions of EXCALIBUR [15], PYTHIA [16], and HERWIG [17] being used to assess possible systematic uncertainties on the theoretical prediction.

To extract the CC03 cross section from the data, the expected difference between the complete four-fermion production rate and the rate predicted using only the CC03 diagrams is treated as a background and subtracted from the observed cross section. This four-fermion background is estimated using the KORALW, EXCALIBUR, and grc4f [18] four-fermion Monte Carlo generators,[1] and includes contributions from both non-CC03 four-fermion final states and interference between the CC03 and non-CC03 amplitudes. For the $\ell\nu\ell\nu$ final states, where this additional non-CC03 four-fermion contribution is most pronounced, inclusive four-fermion cross sections are also quoted following a signal definition described in Section 7.

Additional backgrounds from two-fermion final states are estimated using the PYTHIA, HERWIG, and KK2f [19] Monte Carlo generators for the $e^+e^- \to q\overline{q}$ process, KORALZ [20] for the $e^+e^- \to \mu^+\mu^-$, $e^+e^- \to \tau^+\tau^-$, and $e^+e^- \to \nu\overline{\nu}\gamma(\gamma)$ processes, and BHWIDE [21] for the $e^+e^- \to e^+e^-$ process. Backgrounds from two-photon interactions are evaluated using PYTHIA, HERWIG, PHOJET [22], and the Vermaseren program [23].

3 $W^+W^- \to \ell^+\nu_\ell\ell'^-\overline{\nu}_{\ell'}$ Event Selection

Fully leptonic W^+W^- events are identified as a pair of charged leptons with significant missing transverse momentum. In previous OPAL results [3, 4], events were considered as $W^+W^- \to \ell^+\nu_\ell\ell'^-\overline{\nu}_{\ell'}$ candidates if they were selected by either of two independent selection algorithms. For the results presented in this paper, however, an improved version of the OPAL acoplanar di-lepton selection II presented in references [24, 25] is used exclusively. The new selection has an efficiency of 82% for W^+W^- events at $\sqrt{s} = 189$ GeV (was approx 72% for selection II in [24]) and a background of 38 fb (was 66 fb in [25]). The main improvements are as follows:

- simplifying the kinematic cuts such that they are lepton flavor independent and based primarily on requirements of significant missing transverse momentum (p_{T});
- using the recently installed forward scintillating tile counters [26] to efficiently reject backgrounds from otherwise undetected forward muons;
- requiring that the measured missing p_{T} could not easily be faked by mis-measurements of the track momenta.

[1] The KORALW four-fermion generator uses the grc4f four-fermion matrix elements, but other details of the event generation differ.

Since the characteristic $\ell\nu\ell\nu$ topology is shared by other non-CC03 Standard Model processes as well as many manifestations of new physics beyond the Standard Model, no attempt has been made in this selection to discriminate CC03 production from other sources. Rather, the selection is developed to be globally efficient for any mechanism which produces two charged leptons and missing transverse momentum in the final state while rejecting the main backgrounds from two-fermion production and two-photon interactions.

To be selected as $\mathrm{W^+W^-} \to \ell^+\nu_\ell\ell'^-\overline{\nu}_{\ell'}$ candidates, events must pass a series of cuts designed to isolate the signal events while rejecting the dominant backgrounds. After rejecting all high multiplicity events, "jets" are found in each candidate event using a cone algorithm applied to the observed tracks and calorimeter clusters. A cone half-opening angle of 20 degrees and a jet energy threshold of 2.5 GeV is used. Only those events with between one and three identified jets are considered further, and a different series of additional cuts is applied depending upon the number of jets observed.

In the most common di-jet case, where the charged lepton candidates are cleanly separated from each other, the most important cuts require a minimum acollinearity angle between the two leptons ($\theta_{\mathrm{acol}} > 5^\circ$), and a minimum scaled transverse momentum ($x_{\mathrm{T}} = p_{\mathrm{T}}/E_{\mathrm{beam}} > 5\%$). Many additional cuts are applied to reject specific background processes, including the rejection of events with significant activity in the forward scintillating tile counters consistent with an otherwise undetected forward muon from $\mathrm{e^+e^-}\mu^+\mu^-$ production.

The tri-jet selection is designed to retain efficiency for $\ell\nu\ell\nu\gamma$ final states where the photon forms a third jet, with additional cuts applied to reject two-fermion $\tau^+\tau^-\gamma$ production. The mono-jet selection is designed to select additional events where both leptons are reconstructed within the same cone, or where one lepton is only partially reconstructed in the forward direction. Tighter cuts are required on x_{T} to suppress backgrounds from two-photon interactions, and event timing cuts are used to eliminate backgrounds from cosmic rays entering the detector.

The classification of the selected $\ell\nu\ell\nu$ events into di-lepton class is initially based on the observed lepton properties, as well as the observed track multiplicity in each jet. This classification is further refined by momentum cuts dependent upon the acollinearity angle such that identified e or μ leptons with low momentum consistent with $\tau \to \ell\nu_\ell\nu_\tau$ decays are reclassified as τ lepton candidates. These cuts are effective due to the correlation between lepton energy and decay angle from the parent W boson.

The inclusive $\ell\nu\ell\nu$ selection is estimated to be $(82.1 \pm 1.2)\%$ efficient for $\mathrm{W^+W^-} \to \ell^+\nu_\ell\ell'^-\overline{\nu}_{\ell'}$ events, where the error indicates the systematic uncertainty. The detailed efficiency matrix listing the selection efficiency of each di-lepton selection class for a specific $\mathrm{W^+W^-} \to \ell^+\nu_\ell\ell'^-\overline{\nu}_{\ell'}$ event type is shown in Table 1. A correction of $(-0.9 \pm 0.4)\%$ has been applied to the efficiency predicted by KORALW Monte Carlo samples to account for unmodelled beam-related backgrounds in the forward detectors. Since significant activity in the forward detectors is used as a veto against various background classes, like the rejection of $\mathrm{e^+e^-}\mu^+\mu^-$ mentioned above, this beam-related detector occupancy causes a reduction of the selection efficiency which is estimated from randomly triggered beam crossings. A variety of other possible systematic effects have been considered including the dependence on W mass, beam energy, trigger efficiency, and several aspects of the detector modeling in the Monte Carlo simulation. All are found to be small ($< 0.4\%$ each), and a total relative uncertainty on the selection efficiency of 1.5% is assessed. This systematic uncertainty is small compared to the expected statistical errors.

Backgrounds to the $\ell\nu\ell\nu$ event selection can be grouped into three distinct classes. The first class consists of backgrounds from processes which do not contain two leptons and two neutrinos in

the final state. Predominantly τ-pair and two-photon ($e^+e^-\ell^+\ell^-$) production, this background class contributes an expected 38 ± 10 fb to the total selected $\ell\nu\ell\nu$ rate. The second class consists of an irreducible background from $\ell^+\ell^-\nu_{\ell'}\overline{\nu}_{\ell'}$ final states which can only be produced by neutral current diagrams as the neutrinos are of a different lepton species than the charged leptons. Since the neutrinos are unobserved, these final states are indistinguishable from the signal events in terms of the event topology. This class contributes an additional 45 ± 2 fb of background to the inclusive $\ell\nu\ell\nu$ selection. The final class of background is the difference between the complete four-fermion cross section and the theoretically predicted rate from CC03 diagrams alone for $\ell\nu\ell\nu$ final states. This includes neutral-current processes in the final states where the two charged leptons are of the same type ($\ell^+\nu_\ell\ell^-\overline{\nu}_\ell$) and other four-fermion processes when there is an electron in the final state ($e^\pm\nu_e\ell^\mp\nu_\ell$). This non-CC03 production contributes a large cross section of 77 ± 10 fb which is treated as a background in the CC03 selection and is also largely irreducible within the detector acceptance. The errors on the accepted background rates include all systematic uncertainties, including the effects of limited Monte Carlo statistics. A detailed breakdown of the accepted background cross-sections for the six di-lepton classes identified in the $\ell\nu\ell\nu$ selection is shown in Table 2.

The dominant systematic uncertainty associated with the $\ell\nu\ell\nu$ background estimate is due to the four-fermion correction. The accepted four-fermion background rate is estimated from the difference observed in KORALW four-fermion and CC03 samples with equivalent EXCALIBUR samples providing a cross-check. The accepted background rates from all processes for the $\ell\nu\ell\nu$ event selection are shown in Tables 2 and 3.

A total of 276 events are selected in the data, with 29 ± 3 expected from all background classes. Figure 2 shows distributions of the reconstructed visible energy fraction for the six individual di-lepton classifications.

4 $W^+W^- \to q\overline{q}\ell^\pm\nu_\ell$ Event Selection

The $W^+W^- \to q\overline{q}\ell^\pm\nu_\ell$ selection consists of three separate selections, one for each type of semi-leptonic decay. Only those events which are not already selected as $W^+W^- \to \ell^+\nu_\ell\ell'^-\overline{\nu}_{\ell'}$ candidates are considered by these selections, and the $W^+W^- \to q\overline{q}\tau\nu_\tau$ selection is only applied to those events which fail both the $W^+W^- \to q\overline{q}e\nu_e$ and $W^+W^- \to q\overline{q}\mu\nu_\mu$ selections.

The $W^+W^- \to q\overline{q}\ell^\pm\nu_\ell$ event selection for the 189 GeV data is based on that described in detail in previous publications [3, 4]. The selection consists of five stages, which can be summarized as

- a loose preselection to remove events with low multiplicity or little visible energy;
- identification of the observed track in the event most consistent with being the leptonic decay of a W boson;
- separate likelihood selections for $W^+W^- \to q\overline{q}e\nu_e$, $W^+W^- \to q\overline{q}\mu\nu_\mu$, and $W^+W^- \to q\overline{q}\tau\nu_\tau$;
- re-classification of $q\overline{q}\tau\nu_\tau$ events which are identified by the $q\overline{q}e\nu_e$ and $q\overline{q}\mu\nu_\mu$ selections;
- rejection of four-fermion backgrounds.

The first three stages are optimized for the rejection of the $e^+e^- \to q\overline{q}$ background which has an expected cross section about six times larger than the W-pair production cross section at 189 GeV. The

$W^+W^- \to q\overline{q}\ell^{\pm}\nu_\ell$ likelihood selections have a significant efficiency for other four-fermion processes, *e.g.* $q\overline{q}e\nu_e$ final states produced by the single W ($We\nu_e$) diagrams and $q\overline{q}\ell^+\ell^-$production. For this reason additional cuts are applied to events passing the likelihood selections to reduce backgrounds from these processes.

The four-fermion background rejection consists of three separate parts. Firstly, cuts are applied to selected $W^+W^- \to q\overline{q}e\nu_e$ and $W^+W^- \to q\overline{q}\mu\nu_\mu$ events to reduce backgrounds from $q\overline{q}e^+e^-$ and $q\overline{q}\mu^+\mu^-$ final states where both leptons are observed in the detector. Secondly, the $W^+W^- \to q\overline{q}\tau\nu_\tau$ selection accepts approximately 40% of hadronically decaying single W events ($q\overline{q}e\nu_e$) where the electron is produced in the far forward region beyond the experimental acceptance. In these events a fragmentation track is mis-identified as a τ lepton decay product. To reduce this background, an additional likelihood selection is applied which separates $W^+W^- \to q\overline{q}\tau\nu_\tau$ from $We\nu_e$. Finally, background in the $W^+W^- \to q\overline{q}e\nu_e$ selection from the Ze^+e^- final state, where the Z^0 decays hadronically and one electron is far forward, is reduced with two kinematic fits, the first using the hypothesis that the event is $W^+W^- \to q\overline{q}e\nu_e$ and the second using the Ze^+e^- hypothesis.

In addition to the likelihood selections, cut based selections are used to identify $W^+W^- \to q\overline{q}e\nu_e$ and $W^+W^- \to q\overline{q}\mu\nu_\mu$ events where the lepton track is either poorly reconstructed or is beyond the tracking acceptance. These 'trackless' selections require clear evidence of an electron or muon in the calorimeter or muon chambers consistent with the kinematics of a $W^+W^- \to q\overline{q}\ell^{\pm}\nu_\ell$ event, without explicitly demanding a reconstructed track. These additional selections improve the overall efficiency by approximately 3% (5%) for $W^+W^- \to q\overline{q}e\nu_e$ ($W^+W^- \to q\overline{q}\mu\nu_\mu$) events, while reducing the systematic uncertainties associated with the modeling of the forward tracking acceptance.

The inclusive $qq\ell\nu$ selection is estimated to be $(86.8 \pm 0.9)\%$ efficient for $W^+W^- \to q\overline{q}\ell^{\pm}\nu_\ell$ events, as predicted by KORALW Monte Carlo samples. The efficiencies of the $W^+W^- \to q\overline{q}\ell^{\pm}\nu_\ell$ selection for the individual channels are given in Table 1. These efficiencies include small corrections (0.5%) which account for observed differences between data and the Monte Carlo simulation. These corrections are obtained using 'mixed events' formed by superimposing $Z^0 \to q\overline{q}$ multihadronic events and hemispheres from $Z^0 \to \ell^+\ell^-$ lepton pairs recorded at $\sqrt{s} = 91$ GeV as described previously [3]. Small corrections (0.3%) are also applied to account for tracking losses which are not modeled by the Monte Carlo simulation of the OPAL detector. These corrections are determined by studying $Z^0 \to \ell^+\ell^-$ events. The effect of detector occupancy from beam-related backgrounds has also been evaluated.

Possible biases due to hadronization uncertainties are studied with fully simulated Monte Carlo $W^+W^- \to q\overline{q}\ell^{\pm}\nu_\ell$ samples where the hadronization process is modeled using either JETSET or HERWIG. Other systematics are evaluated by comparing samples generated with different Monte Carlo generators (KORALW, PYTHIA, EXCALIBUR, and grc4f). In each case, the largest observed difference between generators is taken as an estimate of the systematic uncertainty. Table 5 lists the various contributions to the systematic uncertainty on the selection efficiency.

Table 3 shows the background cross sections and total uncertainties for the three $qq\ell\nu$ selections. The systematic errors on the expected background cross sections are dominated by differences between data and Monte Carlo for the two-fermion backgrounds and by differences between generators in the case of the four-fermion backgrounds. The systematic errors on the four-fermion backgrounds were estimated by comparing the expectations of KORALW and EXCALIBUR.

The dominant background in the $qq\ell\nu$ selection is from di-jet production, predominantly the $e^+e^- \to q\overline{q}$ and single W processes, where a particle produced during hadronization is incorrectly identified as a prompt lepton. The Monte Carlo estimate of this background rate is checked using control samples constructed from the data directly. For the $e^+e^- \to q\overline{q}$ background, 'fake' events

are constructed by boosting hadronic Z^0 events recorded at $\sqrt{s} = 91$ GeV to the $\sqrt{s'}$ distribution expected of quark pairs at $\sqrt{s} = 189$ GeV. This boost procedure is applied to both Z^0 data and Z^0 Monte Carlo samples, with the ratio of selected events in each $q\bar{q}\ell\nu$ channel being used to assign a systematic uncertainty of 15%. For the $We\nu_e$ and $q\bar{q}\nu\bar{\nu}$ backgrounds, which are large in the $q\bar{q}\tau\nu_\tau$ channel, a control sample is constructed from selected $q\bar{q}\ell^{\pm}\nu_\ell$ events by discarding the selected lepton track. Again, the observed ratio in selected events between data and Monte Carlo samples is used to assign a systematic uncertainty of 10% to this background source.

The numbers of events selected in the individual $W^+W^- \to q\bar{q}\ell^{\pm}\nu_\ell$ lepton classes are summarized in Table 4, with a total of 1246 events selected as inclusive $W^+W^- \to q\bar{q}\ell^{\pm}\nu_\ell$ candidates and 112 ± 10 expected from non-CC03 background sources. Figure 3 shows distributions of the reconstructed energy of the lepton in the $q\bar{q}e\nu_e$, $q\bar{q}\mu\nu_\mu$, and $q\bar{q}\tau\nu_\tau$ selection channels. The data distributions are in good agreement with the Monte Carlo expectations.

5 $W^+W^- \to q\bar{q}q\bar{q}$ Event Selection

The selection of fully hadronic $W^+W^- \to q\bar{q}q\bar{q}$ events is performed in two stages using a cut-based preselection followed by a likelihood selection procedure similar to that used at 183 GeV [4]. This likelihood selection is primarily designed to reject the dominant background from the $e^+e^- \to q\bar{q}$ process where the di-quark system fragments into a four jet topology. The changes from this previous selection are a different set of variables used for the preselection cuts and likelihood calculation, and a new method based on data for determining the accepted background rate. No attempt is made to discriminate against the neutral current process $ZZ \to q\bar{q}q\bar{q}$.

All events which are classified as hadronic [27] and which have not been selected by either the $\ell\nu\ell\nu$ or the $qq\ell\nu$ selections are considered as candidates for the $W^+W^- \to q\bar{q}q\bar{q}$ selection. In addition, any event which was rejected as a four-fermion background event in the $qq\ell\nu$ selection is also rejected as a $q\bar{q}q\bar{q}$ candidate event.

Tracks and calorimeter clusters are combined into four jets using the Durham algorithm [28] and the total momentum and energy of each jet is corrected for double-counting of energy [29]. To remove events which are clearly inconsistent with a fully hadronic W^+W^- decay, candidate events are required to satisfy a set of preselection cuts including a cut on minimum visible energy (70% of $\sqrt{s}$), minimum invariant mass (75% of $\sqrt{s}$), and minimum multiplicity per jet (one track). The most important preselection cut is a limit on the logarithm of the QCD matrix element for four jet production ($\log_{10}(W_{420}) < 0$) [30]. W_{420} is an event weight formed from the tree level $\mathcal{O}(\alpha_s^2)$ matrix element [31] for the four jet production process ($e^+e^- \to q\bar{q} \to q\bar{q}q\bar{q}, q\bar{q}gg$). The value of W_{420} is determined by using the observed momenta of the four reconstructed jets as estimates of the underlying parton momenta which are input to the matrix element calculation. The largest value of this matrix element calculated after considering all 24 permutations of the jet-parton association in each event is found to have the best discriminating power between signal and background.

The preselection requirements reject an estimated 96% of the $e^+e^- \to q\bar{q}$ events which comprise the dominant source of background in the $W^+W^- \to q\bar{q}q\bar{q}$ event selection. The preselection efficiency for the hadronic $W^+W^- \to q\bar{q}q\bar{q}$ decays is estimated to be 93%. A total of 2077 data events pass the preselection, of which 775 are expected to be from non-CC03 sources.

Events satisfying the preselection cuts are classified as signal or background based upon a four variable likelihood selection. The following likelihood variables are selected to provide a good sepa-

ration between the hadronic $W^+W^- \to q\overline{q}q\overline{q}$ signal and the $e^+e^- \to q\overline{q}$ four jet background, while minimizing the total number of variables used:

- $\log_{10}(W_{420})$, the QCD four jet matrix element;
- $\log_{10}(W_{\rm CC03})$, the EXCALIBUR matrix element [15] for the CC03 process ($W^+W^- \to q\overline{q}q\overline{q}$);
- $\log_{10}(y_{45})$, the logarithm of the value of the Durham jet resolution parameter at which an event is reclassified from four jets to five jets;
- event sphericity.

Figure 4 shows the distribution of these four likelihood variables for all preselected events found in the 189 GeV data. To improve the statistical power of this selection, a multi-dimensional likelihood technique is used to account for the correlations between the four likelihood input variables [32]. Most of the separation between the signal and background events is provided by the two matrix element values $\log_{10}(W_{\rm CC03})$ and $\log_{10}(W_{420})$, which give the relative probability that the kinematics of the observed event are consistent with signal or background production respectively.

An event is selected as a hadronic $W^+W^- \to q\overline{q}q\overline{q}$ candidate if the likelihood discriminant variable, also shown in Figure 4, is greater than 0.4. This cut value was chosen to maximize the expected statistical power of this selection assuming the Standard Model rate for CC03 production. The efficiency of this likelihood selection for $W^+W^- \to q\overline{q}q\overline{q}$ events is estimated from KORALW Monte Carlo samples to be $(86.4 \pm 0.9)\%$, where the error represents an estimate of the systematic uncertainties. The individual components of this systematic uncertainty are shown in Table 5.

For the purposes of extracting a cross section, an alternative technique of weighting all preselected events according to the likelihood output is employed rather than selecting specific events by making a cut. A similar method was used in previous results [3], although in this analysis the weights (w_i) are calculated for each bin (i) of the likelihood discriminant from the expected CC03 signal purity in that bin. The cross section can then be expressed in terms of the weighted values of efficiency, background, and observed events as

$$\sigma(q\overline{q}q\overline{q}) = (\frac{1}{\mathcal{L}} \sum_i w_i N_i - \sum_i w_i \sigma_i^{\rm bgd})/(\sum_i w_i \varepsilon_i^{\rm sig}),$$

where $\mathcal{L}$ is the luminosity of the sample. The values N_i, $\varepsilon_i^{\rm sig}$, and $\sigma_i^{\rm bgd}$ are the observed events, signal efficiency, and accepted background respectively in each bin. The statistical uncertainty on the weighted number of events is given by $\sqrt{\sum (w_i)^2 N_i}$, and by using this weighting technique an improvement of 3% in the expected $\sigma(q\overline{q}q\overline{q})$ statistical error is gained. Results for both techniques are presented in Section 6 and Tables 3–5.

The main systematic uncertainty on the selection efficiency results from the modeling of the QCD hadronization process. This uncertainty is estimated by comparing the selection efficiency predicted using the JETSET hadronization model with an alternative model from the HERWIG generator. In addition, the effect of varying the parameters $\sigma_{\rm q}$, b, $\Lambda_{\rm QCD}$, and Q_0 of the JETSET hadronization model by one standard deviation about their tuned values [33] is considered. For these JETSET tune studies, a fast parameterized simulation of the OPAL detector was used. The Monte Carlo modeling of the CC03 signal, including the detector simulation, is further studied by comparing the distributions of the preselection and likelihood variables seen in data with various Monte Carlo estimates. The signal efficiency determined by KORALW is also compared to other generators (EXCALIBUR, PYTHIA, and

grc4f) to test the Monte Carlo description of the underlying hard process. In each case, the observed differences are taken as an estimate of the systematic uncertainty. Possible biases related to final state interactions between the hadronic systems produced by different W bosons have been evaluated for color-reconnection effects [34] and Bose-Einstein correlations [35]. These effects are found to be small, and the total change in predicted selection efficiency when these effects are included in the hadronization model is taken as the systematic uncertainty.

The accepted $e^+e^- \to q\overline{q}$ background is estimated from PYTHIA Monte Carlo samples, with HERWIG and KK2f being used as cross-checks. All of these generators include only $\mathcal{O}(\alpha_s)$ matrix elements for hard gluon emission, and rely upon a parton shower scheme to predict the four jet production rate. It has been suggested that this could lead to errors of up to 10% in the rate of $e^+e^- \to q\overline{q}$ background when compared to a more complete $\mathcal{O}(\alpha_s^2)$ matrix element approach [36]. To reduce the uncertainty on this background estimate, a technique to measure this rate directly from the data has been used in this analysis. By comparing the number of events seen in data and Monte Carlo in the range $(0 < \log_{10}(W_{420}) < 1)$ which would otherwise pass the preselection cuts, the overall four jet rate predicted by the Monte Carlo is normalized to the data. A correction of $(-3.6 \pm 3.2)\%$ is found for the default PYTHIA sample assuming a total $e^+e^- \to q\overline{q}$ production cross section of 98.4 pb, where the uncertainty is the statistical precision of the normalization procedure. The observed data and corrected Monte Carlo expectation in this 'sideband' background region is shown in Figure 4. The expected contamination from CC03 production in this region is less than 3%, resulting in a negligible bias on the extracted CC03 cross section.

Additional uncertainties on the background rate from the modeling of the hadronization process are evaluated in the same manner as the uncertainty on the signal efficiency. The background normalization procedure has been consistently applied during these systematic checks. Uncertainties in the non-CC03 four-fermion background are estimated by comparing the expectations of KORALW, grc4f, and EXCALIBUR. This background is predominantly from the neutral current process $ZZ \to q\overline{q}q\overline{q}$, of which only 15% is in final states with direct interference with the CC03 diagrams. In each case, the single largest difference observed in a set of systematic checks is taken as an estimate of the uncertainty.

A total of 1546 $W^+W^- \to q\overline{q}q\overline{q}$ candidate events are selected by the counting analysis, with an expected non-CC03 background of 325 ± 21 events. Using the weighting technique, 1306 ± 32 weighted events are observed with a weighted background estimate of 287 ± 15 events.

6 W^+W^- Cross Section and W Decay Branching Fractions

The observed numbers of selected W^+W^- events are used to measure the W^+W^- production cross section and the W decay branching fractions to leptons and hadrons. The measured cross section corresponds to that of W-pair production from the CC03 diagrams as discussed earlier. The expected four-fermion backgrounds quoted throughout this paper include contributions from both non-CC03 final states and the effects of interference with the CC03 diagrams. Mis-identified CC03 final states are not included in the background values listed in Table 3, but rather are taken into account by off-diagonal entries in the efficiency matrix shown in Table 1.

Table 4 summarizes the event selections in the three W^+W^- decay topologies. The expected numbers of events assume a center-of-mass energy of 188.635 ± 0.040 GeV, an integrated luminosity of 183.05 ± 0.40 pb^{-1}, and a W^+W^- cross section of 16.26 ± 0.08 pb as predicted by the calculations of YFSWW and RACOONWW.

As in [4], the W^+W^- cross section and branching fractions are measured using data from the ten separate decay channels. Three different fits are performed with all correlated systematic uncertainties taken into account. In the first case $\sigma_{WW}(189\ \mathrm{GeV})$, $\mathrm{Br}(W \to e\nu_e)$, $\mathrm{Br}(W \to \mu\nu_\mu)$, and $\mathrm{Br}(W \to \tau\nu_\tau)$ are extracted under the assumption that

$$\mathrm{Br}(W \to e\nu_e) + \mathrm{Br}(W \to \mu\nu_\mu) + \mathrm{Br}(W \to \tau\nu_\tau) + \mathrm{Br}(W \to q\overline{q}) \quad = \quad 1.$$

In the second fit, the additional constraint of charged current lepton universality is imposed. The results of these branching fraction fits to the 189 GeV data alone are summarized in Table 6 along with the Standard Model expectation, which is estimated to have a theoretical uncertainty of 0.1% [1].

From this second fit, the W^+W^- CC03 production cross sections in each channel can be extracted under the assumption of lepton universality, assuming Standard Model rates for all other processes:

$$\begin{aligned}
\sigma(W^+W^- \to \ell^+\nu_\ell\ell'^-\overline{\nu}_{\ell'}) &= 1.64 \pm 0.11(\mathrm{stat.}) \pm 0.03(\mathrm{syst.})\ \mathrm{pb}, \\
\sigma(W^+W^- \to q\overline{q}\ell^\pm\nu_\ell) &= 7.04 \pm 0.22(\mathrm{stat.}) \pm 0.10(\mathrm{syst.})\ \mathrm{pb}, \\
\sigma(W^+W^- \to q\overline{q}q\overline{q}) &= 7.68 \pm 0.24(\mathrm{stat.}) \pm 0.16(\mathrm{syst.})\ \mathrm{pb}.
\end{aligned}$$

These results are consistent with the Standard Model expectations of 1.72 pb, 7.13 pb, and 7.41 pb respectively. The cross section in the qqqq channel has been determined using the event weight technique described in Section 5. Using the counting method yields a consistent result of $\sigma(W^+W^- \to q\overline{q}q\overline{q}) = 7.70 \pm 0.25 \pm 0.18$ pb.

In the third fit, all W decay branching fractions are fixed to the values predicted by the Standard Model, and the W^+W^- cross section is determined to be

$$\sigma_{WW}(189\ \mathrm{GeV}) = 16.30 \pm 0.34(\mathrm{stat.}) \pm 0.18(\mathrm{syst.})\ \mathrm{pb},$$

consistent with the Standard Model expectation of 16.26 ± 0.08 pb.

7 $e^+e^- \to \ell^+\ell^-\nu\overline{\nu}$ Cross Section Measurement

The fully leptonic event selection has only a small (38 ± 10 fb) contamination of background expected from sources without two leptons and two neutrinos in the final state. It is therefore well suited to measuring the inclusive four-fermion cross-sections for the six charged di-lepton final states which within the Standard Model receive contributions from some or all of the WW, ZZ, $We\nu_e$, Ze^+e^-, and $Z\nu\overline{\nu}$ diagrams and in particular their respective interferences.

The four-fermion $e^+e^- \to \ell^+\ell^-\nu\overline{\nu}$ cross sections are defined in terms of the following kinematic acceptance cuts:

- at least one of the charged leptons is produced with $|\cos\theta| < 0.90$, where the angle θ is the scattering angle between the outgoing lepton and the incoming electron;
- both charged leptons are produced with $|\cos\theta| < 0.99$;
- the invariant mass calculated from the four-momentum balancing the two prompt neutrinos must be greater than 10 GeV, while the transverse momentum of this recoil four-momentum must have $p_T/E_{\mathrm{beam}} > 5\%$.[2]

[2] This definition of the 'visible' system in terms of the recoil from the two neutrinos avoids ambiguities in defining the invariant mass when there is additional photon radiation.

For this theoretical signal definition, τ leptons are treated as stable such that the prompt τ lepton is used in the kinematic acceptance cuts. This signal definition is chosen to approximate the kinematic acceptance of the $\ell\nu\ell\nu$ selection. The efficiency of the inclusive $\ell\nu\ell\nu$ selection for this signal definition is 86%.

A combined fit for the six four-fermion cross sections is performed and summarized in Table 7. The observed cross sections are in good agreement with the Standard Model rates predicted by the KORALW four-fermion generator.

8 Combination with Previous Data

A simultaneous fit to the numbers of $\mathrm{W^+W^-}$ candidate events in the ten identified final states ($\mathrm{e\nu_e e\nu_e}$, $\mu\nu_\mu\mu\nu_\mu$, $\tau\nu_\tau\tau\nu_\tau$, $\mathrm{e\nu_e}\mu\nu_\mu$, $\mathrm{e\nu_e}\tau\nu_\tau$, $\mu\nu_\mu\tau\nu_\tau$, $\mathrm{q\overline{q}e\nu_e}$, $\mathrm{q\overline{q}}\mu\nu_\mu$, $\mathrm{q\overline{q}}\tau\nu_\tau$, and $\mathrm{q\overline{q}q\overline{q}}$) observed by OPAL at center-of-mass energies of 161 GeV, 172 GeV, 183 GeV, and 189 GeV gives the following values for the leptonic branching fractions of the W boson:

$$\begin{aligned}
\mathrm{Br(W \to e\nu_e)} &= 10.46 \pm 0.42(\mathrm{stat.}) \pm 0.14(\mathrm{syst.})\,\% \\
\mathrm{Br(W \to \mu\nu_\mu)} &= 10.50 \pm 0.41(\mathrm{stat.}) \pm 0.12(\mathrm{syst.})\,\% \\
\mathrm{Br(W \to \tau\nu_\tau)} &= 10.75 \pm 0.52(\mathrm{stat.}) \pm 0.21(\mathrm{syst.})\,\%.
\end{aligned}$$

Correlations between the systematic uncertainties at the different energy points have been accounted for in the fit. These results are consistent with the hypothesis of lepton universality, and agree well with the Standard Model prediction of 10.8%. The correlation coefficient for the resulting values of $\mathrm{Br(W \to e\nu_e)}$ and $\mathrm{Br(W \to \mu\nu_\mu)}$ is -0.05. The correlation coefficient for the results of either $\mathrm{Br(W \to e\nu_e)}$ or $\mathrm{Br(W \to \mu\nu_\mu)}$ with the measurement of $\mathrm{Br(W \to \tau\nu_\tau)}$ is -0.25.

A simultaneous fit assuming lepton universality gives

$$\mathrm{Br(W \to q\overline{q})} = 68.32 \pm 0.61(\mathrm{stat.}) \pm 0.28(\mathrm{syst.})\,\%,$$

which is consistent with the Standard Model expectation of 67.5%. Here, the dominant sources of systematic uncertainty are from the uncertainty on the $\mathrm{e^+e^-} \to \mathrm{q\overline{q}}$ background in the $\mathrm{W^+W^-} \to \mathrm{q\overline{q}q\overline{q}}$ channel and the uncertainties on the $\mathrm{W^+W^-} \to \mathrm{q\overline{q}}\ell^\pm\nu_\ell$ and $\mathrm{W^+W^-} \to \mathrm{q\overline{q}q\overline{q}}$ selection efficiencies.

The hadronic branching fraction can be interpreted as a measurement of the sum of the squares of the six elements of the CKM mixing matrix, $|\mathrm{V}_{ij}|$, which do not involve the top quark:

$$\frac{\mathrm{Br(W \to q\overline{q})}}{(1 - \mathrm{Br(W \to q\overline{q})})} = \left(1 + \frac{\alpha_s(M_\mathrm{W})}{\pi}\right) \sum_{i=\mathrm{u,c};\, j=\mathrm{d,s,b}} |\mathrm{V}_{ij}|^2.$$

The theoretical uncertainty of this improved Born approximation due to missing higher order corrections is estimated to be 0.1% [1]. Taking $\alpha_s(M_\mathrm{W})$ to be 0.120 ± 0.005, the branching fraction $\mathrm{Br(W \to q\overline{q})}$ from the 161 – 189 GeV data yields

$$\sum_{i=\mathrm{u,c};\, j=\mathrm{d,s,b}} |\mathrm{V}_{ij}|^2 = 2.077 \pm 0.059(\mathrm{stat.}) \pm 0.027(\mathrm{syst.}),$$

which is consistent with the value of 2 expected from unitarity in a three-generation CKM matrix.

Using the experimental knowledge of the sum, $|\mathrm{V_{ud}}|^2 + |\mathrm{V_{us}}|^2 + |\mathrm{V_{ub}}|^2 + |\mathrm{V_{cd}}|^2 + |\mathrm{V_{cb}}|^2 = 1.048 \pm 0.007$ [9], the above result can be interpreted as a measure of $|\mathrm{V_{cs}}|$ which is the least well determined of these matrix elements:

$$|\mathrm{V_{cs}}| = 1.015 \pm 0.029(\mathrm{stat.}) \pm 0.013(\mathrm{syst.}).$$

The uncertainty in the sum of the other five CKM matrix elements, which is dominated by the uncertainty on $|V_{cd}|$, contributes a negligible uncertainty of 0.004 to this determination of $|V_{cs}|$. A more direct determination of $|V_{cs}|$ is also performed by OPAL in the measurement of the hadronic branching fraction of the W boson to charm quarks [37].

9 Summary

Using 183 pb^{-1} of data recorded by OPAL at a mean center-of-mass energy of $\sqrt{s} = 188.6$ GeV, a total of 3068 W-pair candidate events are selected. The data are used to determine the CC03 production cross section assuming Standard Model decay rates:

$$\sigma_{WW}(189 \text{ GeV}) \quad = \quad 16.30 \pm 0.34(\text{stat.}) \pm 0.18(\text{syst.}) \text{ pb.}$$

The measured W^+W^- production cross section at $\sqrt{s} = 188.6$ GeV is shown in Figure 5, together with the previous OPAL measurements of σ_{WW} at $\sqrt{s} = 161.3$ GeV [2], $\sqrt{s} = 172.1$ GeV [3], and at $\sqrt{s} = 182.7$ GeV [4]. The measured cross sections clearly favor the Standard Model prediction over the model where there is no coupling between the weak gauge bosons, confirming the non-Abelian nature of the electroweak interaction. When combined with previous OPAL measurements under the assumption of lepton universality, the hadronic branching fraction of the W boson is found to be

$$\text{Br}(W \to q\overline{q}) \quad = 68.32 \pm 0.61(\text{stat.}) \pm 0.28(\text{syst.}) \, \%,$$

which is consistent with the Standard Model expectation of 67.5%.

Similar measurements have been made at $\sqrt{s} \leq 189$ GeV by ALEPH [38], DELPHI [39], and L3 [40]. Results consistent with the Standard Model are observed by all four LEP collaborations.

Acknowledgements

We particularly wish to thank the SL Division for the efficient operation of the LEP accelerator at all energies and for their continuing close cooperation with our experimental group. We thank our colleagues from CEA, DAPNIA/SPP, CE-Saclay for their efforts over the years on the time-of-flight and trigger systems which we continue to use. In addition to the support staff at our own institutions we are pleased to acknowledge the
Department of Energy, USA,
National Science Foundation, USA,
Particle Physics and Astronomy Research Council, UK,
Natural Sciences and Engineering Research Council, Canada,
Israel Science Foundation, administered by the Israel Academy of Science and Humanities,
Minerva Gesellschaft,
Benoziyo Center for High Energy Physics,
Japanese Ministry of Education, Science and Culture (the Monbusho) and a grant under the Monbusho International Science Research Program,
Japanese Society for the Promotion of Science (JSPS),
German Israeli Bi-national Science Foundation (GIF),
Bundesministerium für Bildung und Forschung, Germany,
National Research Council of Canada,
Research Corporation, USA,

Hungarian Foundation for Scientific Research, OTKA T-029328, T023793 and OTKA F-023259.

References

[1] Proceedings of CERN LEP2 Workshop, CERN 96-01, Vols. 1 and 2, eds. G. Altarelli, T. Sjöstrand and F. Zwirner.

[2] OPAL Collaboration, K. Ackerstaff *et al.*, Phys. Lett. **B389** (1996) 416.

[3] OPAL Collaboration, K. Ackerstaff *et al.*, Eur. Phys. J. **C1** (1998) 395.

[4] OPAL Collaboration, G. Abbiendi *et al.*, Eur. Phys. J. **C8** (1999) 191.

[5] OPAL Collaboration, K. Ahmet *et al.*, Nucl. Instr. and Meth. **A305** (1991) 275;
OPAL Collaboration, S. Anderson *et al.*, Nucl. Instr. and Meth. **A403** (1998) 326.

[6] OPAL Collaboration, K. Ackerstaff *et al.*, Eur. Phys. J. **C6** (1998) 1.

[7] LEP Energy Working Group, private communication;
LEP Energy Working Group, A. Blondel, *et al.*, Eur. Phys. J. **C11** (1999) 573.

[8] D. Bardin *et al.*, Comp. Phys. Comm. **104** (1997) 161;
D. Bardin *et al.*, Nucl. Phys. B, Proc. Suppl. **37B** (1994) 148.

[9] Particle Data Group, D.E. Groom *et al.*, Eur. Phys. J. **C15** (2000) 1.

[10] W. Beenakker, F. A. Berends and A. P. Chapovsky, Nucl. Phys. **B548** (1999) 3;
A. Denner, S. Dittmaier and M. Roth, Nucl. Phys. **B519** (1998) 39.

[11] S. Jadach, *et al.*, "Precision Predictions for (Un)Stable W^+W^- Pair Production at and Beyond LEP2 Energies," UTHEP-00-0101, hep-ph/0007012, *Submitted to Phys. Lett. B*;
S. Jadach, *et al.*, Phys. Rev. **D61** (2000) 113010.

[12] A. Denner, S. Dittmaier, M. Roth and D. Wackeroth, "Electroweak radiative corrections to $e^+e^- \to W^+W^- \to 4$ fermions in double pole approximation – the RacoonWW approach," BI-TP 2000/06, hep-ph/0006307, *Submitted to Nucl. Phys. B*;
A. Denner, S. Dittmaier, M. Roth and D. Wackeroth, Phys. Lett. **B475** (2000) 127.

[13] J. Allison *et al.*, Nucl. Instr. and Meth. **A317** (1992) 47.

[14] S. Jadach *et al.*, Comp. Phys. Comm. **119** (1999) 272;
M. Skrzypek *et al.*, Comp. Phys. Comm. **94** (1996) 216;
M. Skrzypek *et al.*, Phys. Lett. **B372** (1996) 289.

[15] F.A. Berends, R. Pittau and R. Kleiss, Comp. Phys. Comm. **85** (1995) 437.

[16] T. Sjöstrand, Comp. Phys. Comm. **82** (1994) 74.

[17] G. Marchesini *et al.*, Comp. Phys. Comm. **67** (1992) 465.

[18] J. Fujimoto *et al.*, Comp. Phys. Comm. **100** (1997) 128.

[19] S. Jadach, B.F.L. Ward and Z. Was, "The precision Monte Carlo event generator KK for two-fermion final states in e^+e^-collisions," CERN-TH-99-235, hep-ph/9912214, *Submitted to Comp. Phys. Comm.*;
S. Jadach, B.F.L. Ward and Z. Was, Phys. Lett. **B449** (1999) 97.

[20] S. Jadach *et al.*, Comp. Phys. Comm. **79** (1994) 503.

[21] S. Jadach, W. Placzek, B.F.L. Ward, Phys. Lett. **B390** (1997) 298.

[22] R. Engel and J. Ranft, Phys. Rev. **D54** (1996) 4244;
R. Engel, Z. Phys. **C66** (1995) 203.

[23] J.A.M. Vermaseren, Nucl. Phys. **B229** (1983) 347.

[24] OPAL Collaboration, K. Ackerstaff *et al.*, Eur. Phys. J. **C4** (1998) 47.

[25] OPAL Collaboration, G. Abbiendi *et al.*, Eur. Phys. J. **C14** (2000) 51.

[26] G. Aguillion *et al.*, Nucl. Instr. and Meth. **A417** (1998) 266.

[27] OPAL Collaboration, G. Alexander *et al.*, Z. Phys. **C52** (1991) 175.

[28] N. Brown and W.J. Stirling, Phys. Lett. **B252** (1990) 657.

[29] OPAL Collaboration, M.Z. Akrawy *et al.*, Phys. Lett. **B253** (1990) 511.

[30] S. Catani and M.H. Seymour, Phys. Lett. **B378** (1996) 287.

[31] R.K. Ellis, D.A. Ross and A.E. Terrano, Nucl. Phys. **B178** (1981) 421.

[32] D. Karlen, Comp. in Phys. **12** (1998) 380.

[33] OPAL Collaboration, G. Alexander *et al.*, Z. Phys. **C69** (1996) 543.

[34] T. Sjöstrand and V.A. Khoze, Z. Phys. **C62** (1994) 281; Phys. Rev. Lett. **72** (1994) 28;
L. Lönnblad, Z. Phys. **C70** (1996) 107.

[35] L. Lönnblad and T. Sjöstrand, Eur. Phys. J. **C2** (1998) 165.

[36] S. Moretti and W.J. Stirling, Eur. Phys. J. **C9** (1999) 81.

[37] OPAL Collaboration, G. Abbiendi *et al.*, "A Measurement of the Rate of Charm Production in W Decays," CERN-EP-100, *Submitted to Phys. Lett. B.*

[38] ALEPH Collaboration, R. Barate *et al.*, Phys. Lett. **B484** (2000) 205.

[39] DELPHI Collaboration, P. Abreu *et al.*, Phys. Lett. **B479** (2000) 89.

[40] L3 Collaboration, M. Acciarri *et al.*, Phys. Lett. **B436** (1998) 437.

Event	Efficiencies (%) for $W^+W^- \to$									
Selection	$e^+\nu_e e^-\overline{\nu}_e$	$\mu^+\nu_\mu\mu^-\overline{\nu}_\mu$	$\tau^+\nu_\tau\tau^-\overline{\nu}_\tau$	$e^\pm\nu_e\mu^\mp\nu_\mu$	$e^\pm\nu_e\tau^\mp\nu_\tau$	$\mu^\pm\nu_\mu\tau^\mp\nu_\tau$	$q\overline{q}e\nu_e$	$q\overline{q}\mu\nu_\mu$	$q\overline{q}\tau\nu_\tau$	$q\overline{q}q\overline{q}$
$e^+\nu_e e^-\overline{\nu}_e$	75.5	0.0	1.0	0.1	6.2	0.0	0.0	0.0	0.0	0.0
$\mu^+\nu_\mu\mu^-\overline{\nu}_\mu$	0.0	80.4	0.6	1.2	0.1	6.1	0.0	0.0	0.0	0.0
$\tau^+\nu_\tau\tau^-\overline{\nu}_\tau$	0.5	0.3	46.4	0.4	4.1	5.0	0.0	0.0	0.0	0.0
$e^\pm\nu_e\mu^\mp\nu_\mu$	2.5	0.4	1.2	77.8	6.2	7.2	0.0	0.0	0.0	0.0
$e^\pm\nu_e\tau^\mp\nu_\tau$	8.5	0.0	11.1	3.9	63.0	1.1	0.0	0.0	0.0	0.0
$\mu^\pm\nu_\mu\tau^\mp\nu_\tau$	0.1	6.6	8.3	3.9	0.8	60.6	0.0	0.0	0.0	0.0
$q\overline{q}e\nu_e$	0.0	0.0	0.1	0.0	0.2	0.0	85.4	0.1	3.8	0.0
$q\overline{q}\mu\nu_\mu$	0.0	0.0	0.0	0.0	0.0	0.2	0.1	89.2	4.3	0.1
$q\overline{q}\tau\nu_\tau$	0.0	0.0	0.4	0.0	0.0	0.0	4.5	4.4	68.4	0.8
$q\overline{q}q\overline{q}$	0.0	0.0	0.0	0.0	0.0	0.0	0.0	0.1	0.6	86.4
Weighted	0.0	0.0	0.0	0.0	0.0	0.0	0.0	0.1	0.6	72.3

Table 1: CC03 selection efficiency matrix. For the $W^+W^- \to q\overline{q}q\overline{q}$ selection the efficiencies are listed for both the counting and weighted event selections as described in the text.

Background	Accepted background cross sections (fb)						
Class	e^+e^-	$\mu^+\mu^-$	$\tau^+\tau^-$	$e^\pm\mu^\mp$	$e^\pm\tau^\mp$	$\mu^\pm\tau^\mp$	$\ell^+\ell^-$
Non-$\ell^+\ell^-\nu\overline{\nu}$	0.7	1.1	19.8	1.9	9.6	4.4	37.5
$\ell^+\ell^-\nu_{\ell'}\overline{\nu}_{\ell'}$	6.6	9.1	8.6	4.5	9.9	6.5	45.2
$\ell^+\nu_\ell\ell'^-\overline{\nu}_{\ell'}$(4f - CC03)	10.9	10.0	13.9	9.5	21.5	11.6	77.4
Total Background	18.2	20.2	42.3	15.9	41.0	22.5	160.1

Table 2: Accepted $\ell\nu\ell\nu$ background cross sections listed by selection class. Non-$\ell^+\ell^-\nu\overline{\nu}$ is defined as final states which do not contain two leptons and two neutrinos, while $\ell^+\ell^-\nu_{\ell'}\overline{\nu}_{\ell'}$ are final states only produced by neutral current processes. The (4f - CC03) background is the difference in accepted $\ell\nu\ell\nu$ cross section between complete four-fermion production and CC03-only production for $\ell^+\nu_\ell\ell'^-\overline{\nu}_{\ell'}$ final states.

	Accepted background cross sections (fb)					
	Event Selection $W^+W^- \to$					
Source	$\ell^+\nu_\ell\ell'^-\overline{\nu}_{\ell'}$	$q\overline{q}e\nu_e$	$q\overline{q}\mu\nu_\mu$	$q\overline{q}\tau\nu_\tau$	$q\overline{q}q\overline{q}$	Weighted
$\ell^+\nu_\ell\ell'^-\overline{\nu}_{\ell'}$	77 ± 10	–	–	0 ± 1	–	–
$q\overline{q}\ell^\pm\nu_\ell$	3 ± 1	54 ± 21	2 ± 1	74 ± 8	–	–
$q\overline{q}q\overline{q}$	–	0 ± 1	1 ± 1	13 ± 3	392 ± 67	320 ± 45
$\ell^+\ell^-\nu_{\ell'}\overline{\nu}_{\ell'}$	45 ± 2	–	–	–	–	–
$q\overline{q}\nu\overline{\nu}$	3 ± 1	–	–	32 ± 3	–	–
$q\overline{q}e^+e^-$	1 ± 1	30 ± 7	–	48 ± 12	22 ± 6	19 ± 6
$q\overline{q}\ell^+\ell^-$	–	2 ± 1	28 ± 2	46 ± 4	26 ± 5	22 ± 4
$e^+e^-f\overline{f}$	9 ± 9	7 ± 7	1 ± 1	7 ± 7	2 ± 2	2 ± 2
$\nu\overline{\nu}\gamma(\gamma)$	2 ± 1	–	–	–	–	–
$\ell^+\ell^-$	20 ± 4	2 ± 1	1 ± 1	5 ± 1	–	–
$q\overline{q}$	–	40 ± 8	22 ± 4	192 ± 29	1337 ± 87	1210 ± 62
Combined	160 ± 14	135 ± 24	55 ± 6	417 ± 34	1777 ± 117	1570 ± 84

Table 3: Accepted background cross sections. Backgrounds from non-CC03 sources are shown for the 189 GeV W^+W^- selections. The first three lines list differences in accepted cross sections between a complete four-fermion sample and a CC03 sample for these final states. The $e^+e^-f\overline{f}$ class, containing all additional four-fermion background not explicitly counted elsewhere, is dominated by two-photon interactions. Backgrounds in the qqqq selection are listed for both the counting and weighted event analyses as described in the text. All errors include both statistical and systematic contributions.

Selected as	Observed	Total Expected	Efficiency (%)	Background
$e^+\nu_e e^-\overline{\nu}_e$	37	34.4 ± 1.1	75.5 ± 1.1	3.3 ± 1.0
$\mu^+\nu_\mu\mu^-\overline{\nu}_\mu$	34	37.1 ± 1.1	80.4 ± 1.2	3.7 ± 1.0
$\tau^+\nu_\tau\tau^-\overline{\nu}_\tau$	37	30.9 ± 1.0	46.4 ± 0.7	7.7 ± 1.0
$e^\pm\nu_e\mu^\mp\nu_\mu$	68	68.0 ± 1.3	77.8 ± 1.2	2.9 ± 1.0
$e^\pm\nu_e\tau^\mp\nu_\tau$	46	61.9 ± 1.2	63.0 ± 1.0	7.5 ± 1.0
$\mu^\pm\nu_\mu\tau^\mp\nu_\tau$	54	55.0 ± 1.2	60.6 ± 0.9	4.1 ± 1.0
$q\overline{q}e\nu_e$	389	414.3 ± 6.5	85.4 ± 0.8	25.1 ± 4.4
$q\overline{q}\mu\nu_\mu$	420	418.9 ± 4.8	89.2 ± 0.8	10.1 ± 1.1
$q\overline{q}\tau\nu_\tau$	437	423.6 ± 9.5	68.4 ± 1.4	76.3 ± 6.2
$\ell^+\nu_\ell\ell'^-\overline{\nu}_{\ell'}$	276	287.2 ± 5.0	82.1 ± 1.2	29.3 ± 2.9
$q\overline{q}\ell^\pm\nu_\ell$	1246	1256.8 ± 16.1	86.8 ± 0.9	111.5 ± 9.5
$q\overline{q}q\overline{q}$	1546	1500.0 ± 25.2	86.4 ± 0.9	325.3 ± 21.4
Weighted	1306.1 ± 31.8	1270.5 ± 19.1	72.3 ± 0.7	287.4 ± 15.4
any	3068	3044.0 ± 32.1	86.6 ± 0.6	466.1 ± 23.6

Table 4: Event selection summary. The observed and expected numbers of events for each selection category are shown for an integrated luminosity of 183.05 ± 0.40 pb^{-1} at $\sqrt{s} = 188.635 \pm 0.040$ GeV assuming Standard Model production rates. The expected efficiency of each individual selection for that particular CC03 final state and the expected number of background events from non-CC03 processes is also shown separately. The errors on the expected numbers of events includes the theoretical uncertainty on the predicted W^+W^- production cross section of 16.26 ± 0.08 pb. The inclusive $W^+W^- \to$ any numbers use the counting method in the $q\overline{q}q\overline{q}$ channel. The uncertainties on combined numbers account for all correlations.

	Signal efficiency error (%)				
	Event Selection $W^+W^- \to$				
Source of uncertainty	$q\overline{q}e\nu_e$	$q\overline{q}\mu\nu_\mu$	$q\overline{q}\tau\nu_\tau$	$q\overline{q}q\overline{q}$	Weighted
Statistical	0.18	0.17	0.27	0.06	0.20
Comparison of MC generators	0.24	0.51	0.78	0.21	0.23
Fragmentation	0.40	0.40	0.60	0.72	0.54
M_W dependence	0.01	0.02	0.02	0.05	0.05
Beam energy dependence	0.01	0.02	0.01	0.01	0.01
Tracking losses	0.40	0.10	0.30	0.18	0.15
Final-state interactions	–	–	–	0.36	0.34
Data/MC preselection	0.29	0.24	0.58	–	–
Data/MC likelihood selection	0.36	0.34	0.72	0.12	0.17
Detector occupancy	0.02	0.02	0.02	–	–
Four-fermion rejection	0.30	0.10	0.30	–	–
Total	0.84	0.80	1.44	0.86	0.74

Table 5: Selection efficiency systematic uncertainties. For the $W^+W^- \to q\overline{q}q\overline{q}$ selection the uncertainties are listed for both the counting and weighted event selections. All contributions are listed as the absolute difference in selection efficiency.

Fitted	Fit assumptions:		Standard Model
Parameter	No lepton universality	Lepton universality	Expectation
$Br(W \to e\nu_e)$	$10.03 \pm 0.47 \pm 0.16$ %		10.8%
$Br(W \to \mu\nu_\mu)$	$10.63 \pm 0.47 \pm 0.16$ %	$10.51 \pm 0.23 \pm 0.12$ %	10.8%
$Br(W \to \tau\nu_\tau)$	$10.94 \pm 0.59 \pm 0.25$ %		10.8%
$Br(W \to q\overline{q})$	$68.41 \pm 0.71 \pm 0.36$ %	$68.47 \pm 0.70 \pm 0.35$ %	67.5%

Table 6: Summary of branching fraction results from the OPAL $\sqrt{s} = 188.6$ GeV data alone. The results from the different branching fraction fits described in the text are shown, where the two errors represent the statistical and systematic uncertainties respectively. The leptonic and hadronic branching fractions in each case are not independent, but have been determined assuming that the sum is equal to unity. When assuming lepton universality, small differences in the leptonic branching fractions due to lepton mass effects have been neglected.

$e^+e^- \to$	Measured cross section (fb)	Expected (fb)
$e^+e^-\nu\overline{\nu}$	$290^{+56}_{-51} \pm 11$	262
$\mu^+\mu^-\nu\overline{\nu}$	$195^{+44}_{-40} \pm 08$	221
$\tau^+\tau^-\nu\overline{\nu}$	$290^{+73}_{-66} \pm 13$	207
$e^\pm\mu^\mp\nu\overline{\nu}$	$384^{+60}_{-55} \pm 11$	387
$e^\pm\tau^\mp\nu\overline{\nu}$	$225^{+64}_{-58} \pm 10$	388
$\mu^\pm\tau^\mp\nu\overline{\nu}$	$348^{+69}_{-63} \pm 11$	376

Table 7: Four-fermion $\ell^+\ell^-\nu\overline{\nu}$ cross sections. Observed cross sections are shown for each $\ell\nu\ell\nu$ decay topology using the four-fermion signal definition described in the text. All six cross sections were determined in a simultaneous fit to the observed number of events. The errors shown are the statistical and systematic contributions respectively. The expected cross sections within the Standard Model are calculated using the KORALW four-fermion Monte Carlo generator.

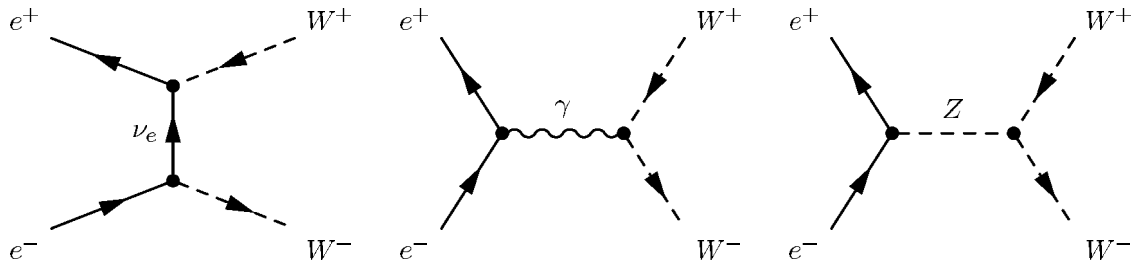

Figure 1: The CC03 diagrams for W-pair production.

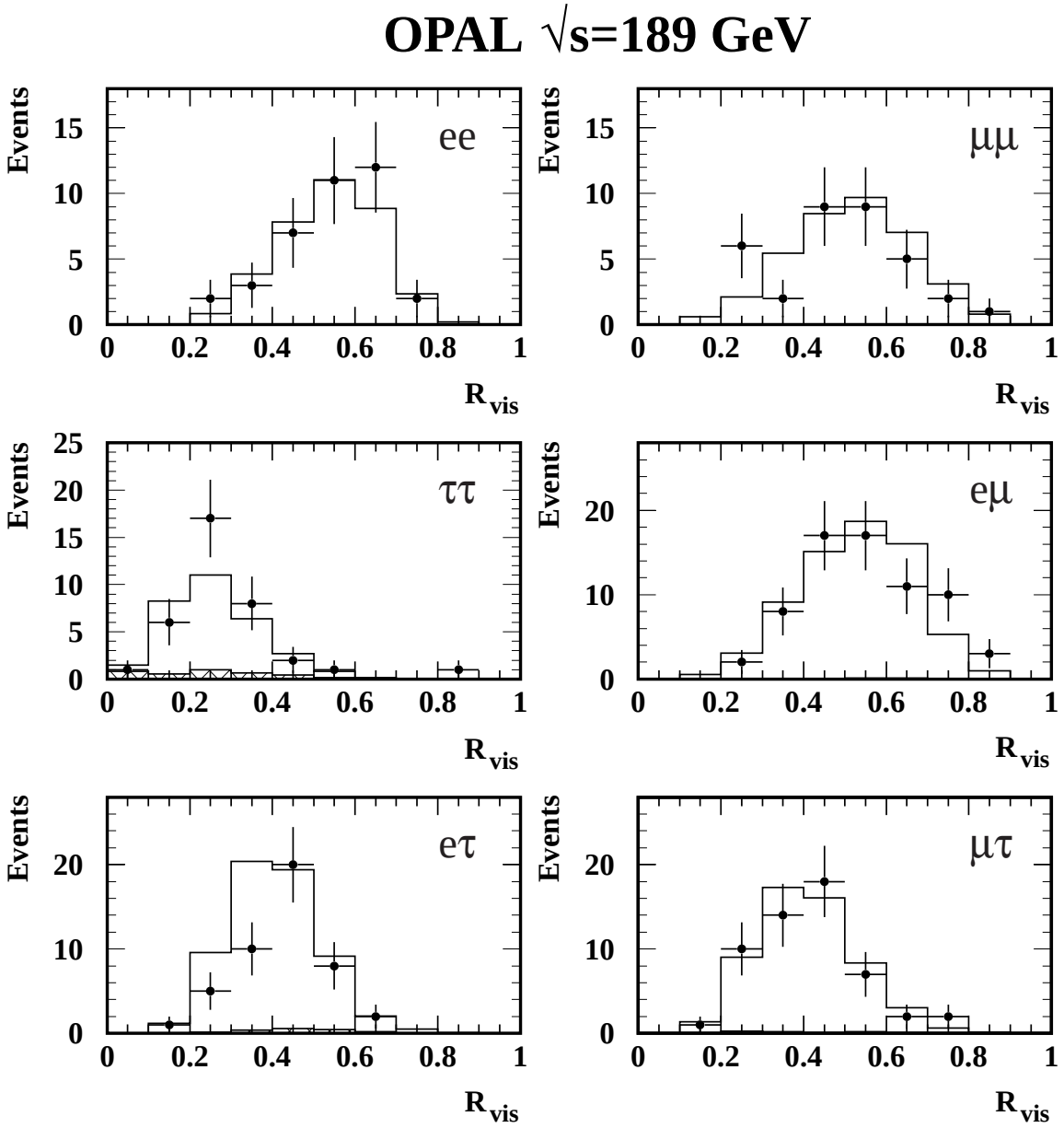

Figure 2: Distributions of visible energy scaled to the center-of-mass energy, $R_{\rm vis}$, for the six di-lepton classes selected as $\mathrm{W^+W^-}\to \ell^+\nu_\ell\ell'^-\overline{\nu}_{\ell'}$. The data are shown as the points with statistical error bars. The total Monte Carlo expectation is shown as the histogram with the non-$\ell^+\ell^-\nu\overline{\nu}$ background contribution shown by the hatched histogram.

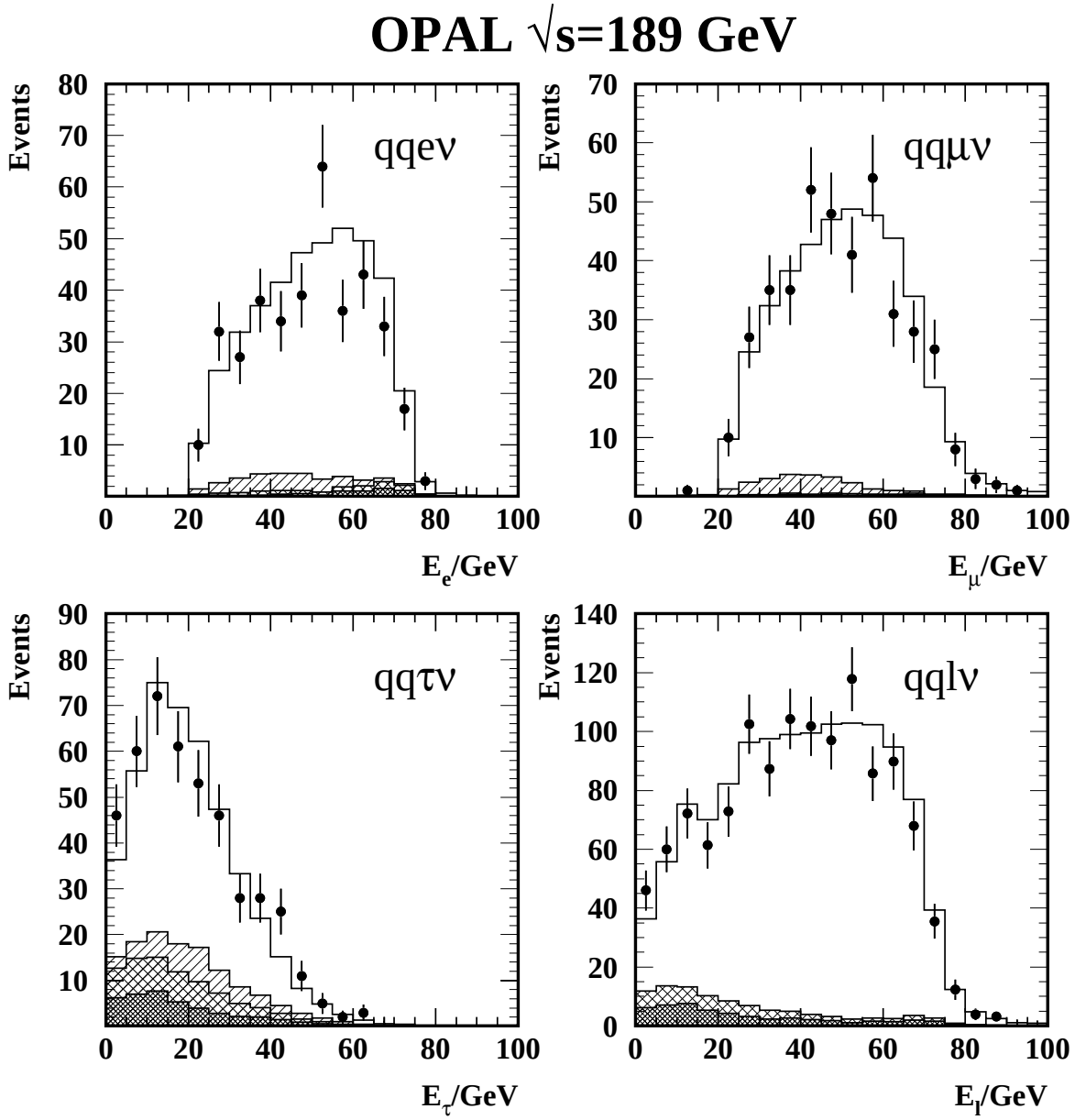

Figure 3: Distributions of measured lepton energy for events selected as $q\bar{q}e\nu_e$, $q\bar{q}\mu\nu_\mu$, and $q\bar{q}\tau\nu_\tau$. Also shown is the combined distribution for all events selected as $W^+W^- \to q\bar{q}\ell^\pm\nu_\ell$. The data are shown as the points with statistical error bars, while the histogram is the total Monte Carlo expectation. The background from two-fermion processes is shown by the dark hatched region, while the non-CC03 four-fermion background is shown by the lighter hatched region. Mis-identified $W^+W^- \to q\bar{q}\ell^\pm\nu_\ell$ events are shown in the individual lepton classifications as the singly hatched histogram.

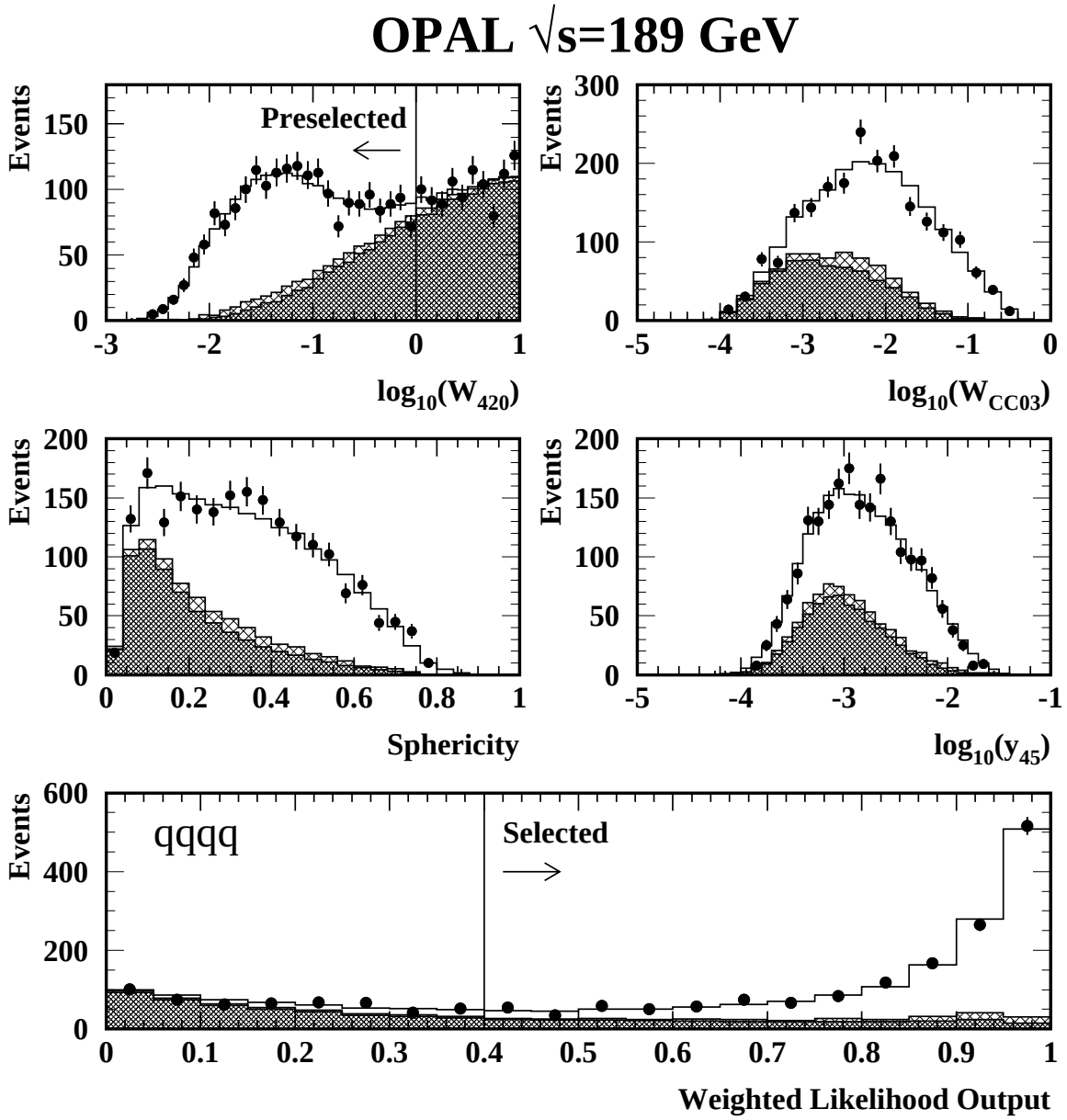

Figure 4: Distributions of the $W^+W^- \to q\bar{q}q\bar{q}$ likelihood selection variables. The four likelihood input variables and resulting likelihood discriminant are shown for all events passing the $W^+W^- \to q\bar{q}q\bar{q}$ preselection. The data are shown as the points with statistical error bars, while the histogram is the total Monte Carlo expectation. The dark hatched region shows the contribution from two-fermion processes, while the light hatched region shows the contribution from non-CC03 four-fermion processes. In the W_{420} distribution, the events used to normalize the $e^+e^- \to q\bar{q}$ background rate are also shown to the right of the vertical line. In the likelihood output distribution, the selection cut used in the counting analysis is indicated by the vertical line, with the selection accepting all events to the right of this cut.

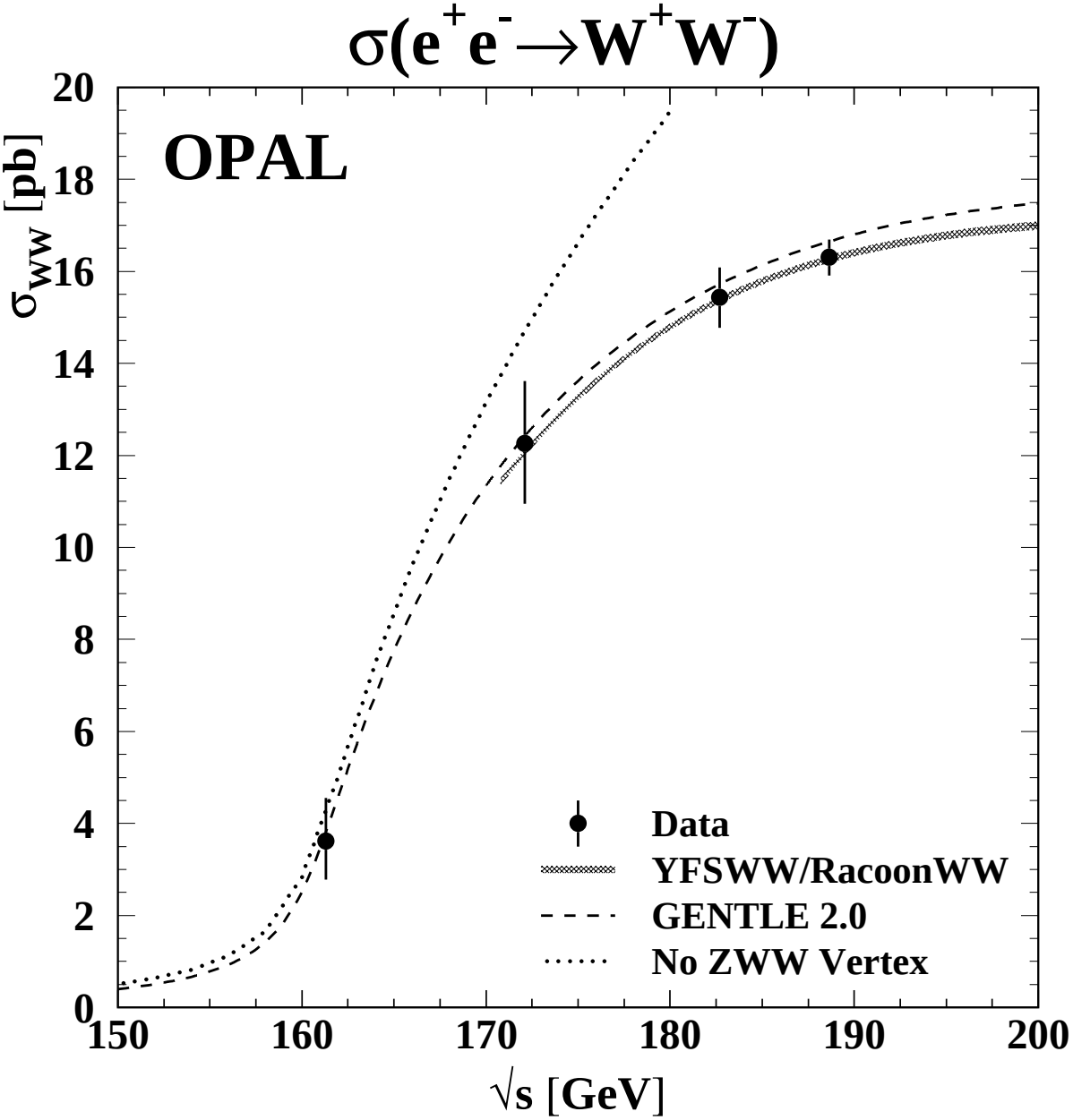

Figure 5: The dependence of σ_{WW} on $\sqrt{s}$. The $\mathrm{W^+W^-}$ cross sections measured at $\sqrt{s} = 188.6$ GeV (this paper), at $\sqrt{s} = 161.3$ GeV[2], at $\sqrt{s} = 172.1$ GeV[3], and at $\sqrt{s} = 182.7$ GeV[4] are shown. The error bars include statistical and systematic contributions. The shaded area shows the prediction of RacoonWW and YfsWW, with the width of the band covering the range of the estimated theoretical uncertainty. The dashed curve shows the older Gentle 2.0 prediction, while the dotted curve indicates the expected cross section if there is no ZWW coupling.